Remittances Review
June 2024,
Volume: 9, No: 3, 2017-2037
ISSN: 2059-6588(Print) | ISSN 2059-6596(Online
Received : 20 April 2024,Accepted: 15 May 2024

Establishing Depth Duration Frequency Curves and Critical Rainfall Thresholds Using Satellite Rainfall Estimates in Data-Scarce Regions: A Case Study of Jammu and Kashmir

Running Title: Development of DDF Curves and Critical Rainfall Thresholds

Azid Shabbir*[1], Muhammad Arshad[1], Muhammad Adnan Shahid[1,2], Syed Aftab Wajid[3]

[1]Department of Irrigation and Drainage, Faculty of Agricultural Engineering and Technology, University of Agriculture, Faisalabad, Pakistan; [2]National Center of GIS and Space Applications – Agricultural Remote Sensing Lab (NCGSA–ARSL), University of Agriculture, Faisalabad, Pakistan; [3]Department of Agronomy, Pakistan University of Agriculture, Faisalabad, Pakistan.

*Corresponding author's e-mail: azidshabbiruaf@gmail.com

Abstract

Climate change has significantly altered rainfall regimes, resulting in recurrent cycles of flooding and drought. Effective flood mitigation and agricultural management now require timely, real-time precipitation alerts. Historically, rainfall has been monitored using ground-based precipitation gauges; however, the spatial density of these stations is low, and their coverage is geographically limited. In recent years, satellite-derived rainfall estimates with enhanced accuracy have become widely available, providing comprehensive coverage across the entire globe. This open-source data offers a superior alternative to the sparsely distributed and often incomplete ground-based gauge records. In this study, rainfall observations from the Global Precipitation Measurement (GPM) Mission and the Tropical Rainfall Measurement Mission (TRMM) were utilized, spanning seventeen years. These datasets enable a more robust assessment of rainfall variability and improve the reliability of hydrological and agricultural analyses.Evaluation of satellite data shows the good results where R^2 values greater than 0.774 for both GPM and TRMM data sets. The other statistical evaluations such as ME, MAE, RMSE, PBias, NSE and r were under acceptable range for both data sets The Generalized Extreme Value (GEV) distribution was used in this study to carry out the statistical analysis. This method helps capture the behaviour of extreme rainfall events more accurately than traditional techniques. Depth–Duration–Frequency (DDF) curves were then developed for selected districts of Kashmir across four time intervals 3 hours, 6 hours, 12 hours, and 24 hours. These curves provide valuable insights for planning, flood risk assessment, and infrastructure design.

Key Words: Climate Change, Rainfall, Global Precipitation Measurement, Depth–Duration–Frequency, Generalized Extreme Value

Remittances Review
June 2024,
Volume: 9, No: 3, 2017-2037
ISSN: 2059-6588(Print) | ISSN 2059-6596(Online

1. Introduction

Water is essential for life's existence on earth; the main sources of water availability on earth are surface water (ocean, rivers, lakes, etc) and groundwater. Rainfall and snowmelt are the major sources of surface water. Water is used for household, commercial, industrial, and agricultural consumption. Floods are natural hazards and cannot be eliminated. The major factors in flood occurrence are heavy rainfall and snowmelt. Rainfall data is used to assess flood alerts and is also used in the structure design for the storage and disposal of excess rainfall water. Among all the meteorological variables, rainfall is the most critical variable. Natural disasters such as floods and droughts occurred due to rainfall events. Intensity varies spatially and temporally(Zhang and Zhou, 2015). This variability, along with land condition and topography, is significant. Climate change alters the rainfall patterns and intensity, and greenhouse gas emissions increase the temperature of the Earth. Climate change caused successive floods and famines (Piman *et al.*, 2016).

The traditional method for rainfall measurement is ground rain gauges. There are two types of rain gauges i.e. recording and non-recording. It requires manual reading daily. In developing countries like Pakistan, rain gauges are the primary source of precipitation data, with very low area coverage in the entire country. There are some disadvantages of this technique, which are a low density of rain gauges, difficulty in installing in the mountains, and not being installed in the oceans. This system required a larger labour force to look after the equipment. Another major disadvantage of rain gauge systems is that they only record the point data, so for proper data collection, a dense network of rain gauges is required. This dense installation of the rain gauges increased the installation and operation costs. Natural hazards like earthquakes and floods may destroy rain gauge stations and cause data loss. For hydrometeorology and climatology, precise long-term rainfall estimates, as well as good spatio-temporal resolution, are required. This needs a good system of rain gauge stations. Lack of a ground rain gauge caused the precipitation unpredictability majorly during the monsoon period. (Prakash, 2019).

Due to climate change, precipitation increased in the high latitudes but did not increase in the low latitudes, which may also shift the monsoon rainfall in some areas of Pakistan. Out of the total rainfall, 60% was received in the monsoon season (June-September). Pakistan is very sensitive to changes in the rainfall patterns; due to the increase in rainfall, northern areas are prone to floods, but the southern areas are highly vulnerable to droughts (Hanif *et al.*, 2013).To overcome the limitations of the land-based rainfall measuring method in the 20th century several metrological satellites have been sent into space to study the different parameters of the atmosphere. These satellites have different sensors on board that can measure different parameters of precipitation. These sensors received the emitted or scattered radiation from the earth and atmosphere. National Oceanic and Atmospheric Administration (NOAA), National Aeronautics and Space Administration (NASA) and a lot of other private and Government Agencies send many satellite missions to space, which enhanced the precipitation data availability. Satellite-based precipitation data has many advantages over ground-based gauge data, e.g. it has better Temporal and Spatial resolution. Satellites also cover the oceans and remote areas. On the other hand, these

satellite data are not sufficiently developed to incorporate into decision-making for water resource management and hydrological reservoirs because this data has many uncertainties (Islam, 2013).

NASA and JAXA (Japan Aerospace Exploration Agency) launched TRMM (Tropical Rainfall Measuring Mission) on November 27th, 1997, for the observation of precipitation and weather parameters on a global scale (Kummerow *et al*., 2000). TRMM provides a lot of information on tropical rainfall and other parameters. It was the first device of this type to feature an on-board precipitation radar and the capability to detect rainfall with the assistance of passive microwave sensors (Kummerow *et al*., 1998)

The precipitation radar of TRMM operates on the Ku band due to its limits in power, weight, and size, along with the fact that it needed narrow beams to get a better resolution at ground level. Therefore, TRMM observation is highly attenuations because of the scattering of hydrometers (Li and Shao, 2010). TRMM precipitation radar records the minimum rainfall intensity of 0.7 mm/hr. TRMM covers 40^0 S and 40^0 N with an angle of 35^0. It has 9 9-hour revisit time. Its revisit time depends on latitude because it is earth low-earth-orbiting satellite. The life span of TRMM was increased in August 2001, with a boost in altitude from 350 km to 403 km https://gpm.nasa.gov/missions/TRMM/satellite/PR.There are three main sensors onboard in TRMM satellite: PR (precipitation radar), which provides the three-dimensional maps of rainfall storms; the second one is TMI (TRMM microwave Imager) is a small sensor that requires small energy, used to measure cloud water, rainfall, and water vapours. VIRS (visual infrared scanner) is one of the three, which is an indirect indicator of rainfall. It measures the cloud coverage and cloud top temperature with high resolution (Kummerow *et al*., 1998). Cloud and Earth's radiant energy system (CERES) and light imaging scanners (LIS) are two more instruments coupled on the TRMM satellite for the measurement of emitted and reflected energy from Earth and distribution of the light intensity over Earth, respectively. GPM (Global Precipitation Measurement Mission) was sent to space on 27th February 2014. The primary objective of this mission was to provide the next-generation global estimates of snow and precipitation. In hydrology, precipitation data has many long-term applications, including flood simulation, storm-water quality criteria, and reservoir design.

Hydro-meteorology and climatology, precise long-term rainfall estimates, as well as good spatio-temporal resolution, are required. This needs a good system of rain gauge stations. Lack of a ground rain gauge caused the precipitation unpredictability majorly during the monsoon period (Prakash, 2019). Due to climate change, precipitation increased in the high latitudes but did not increase in the low latitudes, which may also shift the monsoon rainfall in some areas of Pakistan. Out of the total rainfall, 60% was received in the monsoon season (June-September). Pakistan is very sensitive to the changes in the rainfall patterns; due to the increase in rainfall, northern areas are prone to floods, but the southern areas are highly vulnerable to droughts (Hanif *et al*., 2013).To overcome the limitations of the land-based rainfall measuring method in the 20th century, several meteorological satellites have been sent into space to study the different parameters of the atmosphere. These satellites have different sensors on board that can measure different parameters of precipitation. These

sensors received the emitted or scattered radiation from the earth and atmosphere. National Oceanic and Atmospheric Administration (NOAA), National Aeronautics and Space Administration (NASA), and a lot of other private and Government Agencies send many satellite missions to space, which enhanced the precipitation data availability. Satellite-based precipitation data has many advantages over ground-based gauge data, e.g. it has better Temporal and Spatial resolution. Satellites also cover the oceans and remote areas. On the other hand, these satellite data are not sufficiently developed to incorporate into decision-making for water resource management and hydrological reservoirs because this data has many uncertainties (Islam, 2013).

In Maryland, USA, which used TTMM multi-satellite precipitation analysis (TMPA) data and rain gauge data having $.25^{o}$x$.25^{o}$ spatial and 3 hr temporal resolution. The statistical results, bias values range between 7.1 to 16.6, and root mean square error lies between 35.4 to 42.2, which shows TMPA has high efficiency in estimating rainfall as compared to ground rain gauges Huffman *et al.*(2007) .In Brazil, to evaluate the TRMM precipitation estimates with both rain gauge and merged satellite and rain gauge data from GPCP. Statistical analysis was performed on TRMM data, with a 99% confidence interval result indicating a fine correlation with the seasonal bias. Results showed that during the month of DJF, TRMM underestimates the rainfall with a higher root mean square error than GPCP. It is observed that the satellite data showed consistent results for the months of MAM. It was recommended that the TRMM data provide reliable estimates so it may be used for the area of the sparse rain gauge network, Franchino *et al.* (2009).
The accuracy of three different satellite precipitation products named PERSIANN, CMORPH, and TMPA – 3B42RT by comparing with the grid cell mean rainfall based on ground rain gauge measurements in Indonesia. All three products underestimate during the dry months. PERSIANN and CCMORPH do not match the gauge data and also differ from the TMPA product. Statistical analysis was performed to calculate the relative bias; corrected bias was used to develop an equation of a power law, which is uniform in both space and time against each estimation. For all regions, these bias-corrected data reduced the root mean square error for the dry season by a mean 9% (from 40mm to 44mm) and annually by 14% (from 66 mm to 77 mm). They recommended that the corrected TMPA 3B42RT product is preferred for real-time drought monitoring in Indonesia Vernimmen *et al.* (2012) .

NASA and JAXA (Japan Aerospace Exploration Agency) launched TRMM (Tropical Rainfall Measuring Mission) on November 27th, 1997, for the observation of precipitation and weather parameters on a global scale (Kummerow *et al*., 2000). TRMM provides a lot of information on tropical rainfall and other parameters. It was the first device of this type to feature an on-board precipitation radar and the capability to detect rainfall with the assistance of passive microwave sensors (Kummerow *et al.*, 1998).

Many statistical estimation techniques are used for estimating the parameters of a distribution to get the best fit by optimizing the data-dependent variable/function. Normally whole data is used to estimate these parameters for the base function. A different function is used when someone is interested in modelling extreme values. GEV (Generalized Extreme Value) is a distribution that successfully models the extreme values.

GEV distribution most popular probability distribution that has many applications in distribution and often shows satisfactory results Coles, 2001).

Remittances Review
June 2024,
Volume: 9, No: 3, 2017-2037
ISSN: 2059-6588(Print) | ISSN 2059-6596(Online

2. MATERIALS AND METHODS

2.1 Study Area:

Kashmir is a mountainous region known for its diverse landscape, which includes the foothills of the Himalayas, lush valleys, and major rivers such as the Jhelum and Neelum. The highest peak in the area is Sarwaali Peak in the Neelum Valley, rising to 6,326 meters. The region experiences a varied climate, with heavy summer and winter rainfall, and it is particularly prone to flooding during the monsoon season. Kashmir is a self-governed territory divided into two main administrative divisions: Muzaffarabad and Poonch. .

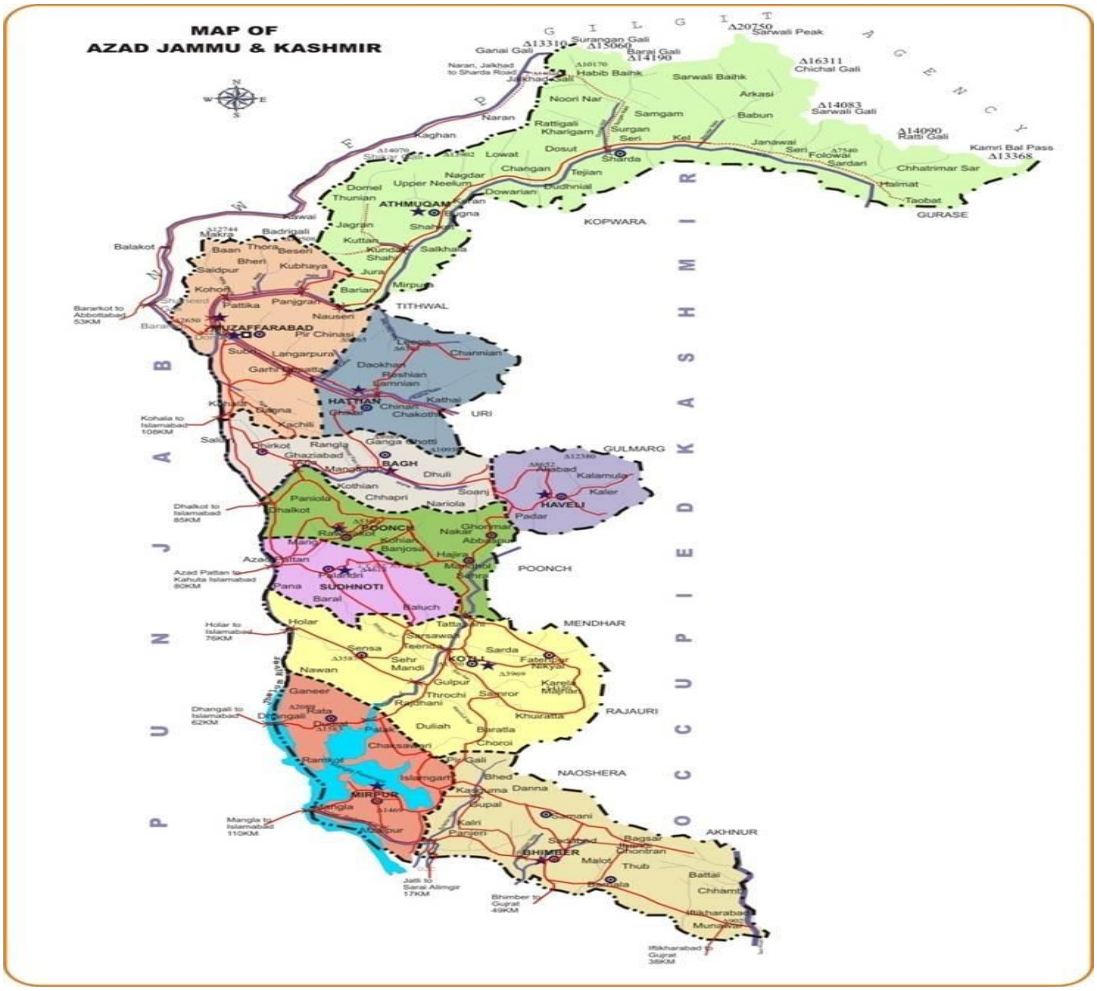

Figure 2.1: Study Area Map

2.2 Data Collection:

The study used precipitation measurements from ground-based rain gauges, along with satellite-derived rainfall estimates. For this study, ground-based precipitation measurements were obtained from the Pakistan Meteorological Department. These observational datasets served as a primary source of reliable, high-resolution rainfall information for the designated study area. The Global Precipitation Measurement (GPM) mission provides satellite-based precipitation observations. In this study, the TRMM and

GPM precipitation product with hourly temporal resolution was utilized for the designated study area.

2.3 Frequency Analysis:

Frequency analysis was conducted to estimate rainfall depths corresponding to specific return periods or exceedance probabilities. For this purpose, historical rainfall records spanning a sufficiently long period were collected and analysed.For this study rainfall data from 2003 to 2019 was used to develop the Depth Duration Frequency curves for each district of Kashmir.

2.4 Generalized Extreme ValaueDistribution:

The GEV distribution is a robust statistical model for extreme rainfall events, allowing estimation of rainfall depths for specific return periods. These estimates are then used to develop DDF curves, which are crucial for hydrological design and flood risk management.

GEV distribution equation is given below

$$G(x) = \exp\left\{-\left[1 + \frac{\xi(x-\mu)}{\delta}\right]^{-1/\xi}\right\}$$

Where ξ (shape) ,μ (location) and δ (scale)

When ξ≠0 and $\left[1 + \frac{\xi(x-\mu)}{\delta}\right]$>0

If ξ = 0 GEV equation is written as

$$G(x) = \exp\left\{-\exp\left(\frac{\xi(x-\mu)}{\delta}\right)\right\}$$

2.5 Graphical representation of GEV Distribution

Plot the PDF of the GEV distribution for various values of the shape parameter (ξ).

Remittances Review
June 2024,
Volume: 9, No: 3, 2017-2037
ISSN: 2059-6588(Print) | ISSN 2059-6596(Online

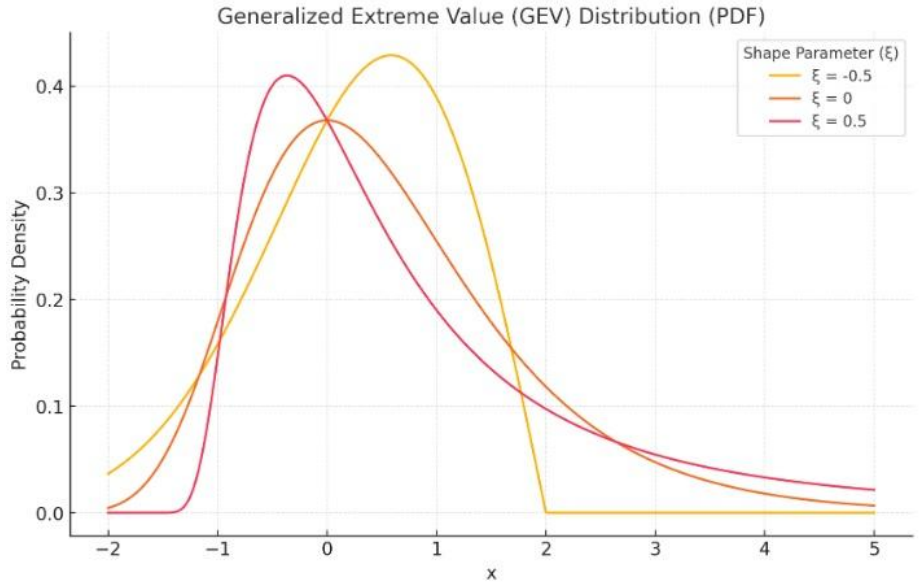

Figure 2.2: Graphical representation of GEV distribution

The graph shows the Probability Density Function (PDF) of the Generalized Extreme Value (GEV) distribution for different shape parameters (ξ): The Weibull distribution is left-skewed and has a finite upper limit (ξ = -0.5). ξ = 0 ξ=0 (Gumbel type): The distribution is light-tailed, symmetric, and without finite limits. The Frechet distribution (ξ = 0.5, ξ = 0.5) is ideal for representing extreme values with considerable variability due to its thick right tail. The GEV distribution is adaptable and can accommodate many forms of extreme value data.

2.6 Fitting the Distribution

Once the annual maxima precipitation depths of 3, 6, 12, and 24-hours duration have been collected, the next step is to perform an appropriate frequency analysis on this date. There are many tools like MATLAB, MS Excel, Easyfit, R and SAS, etc. that can be used to perform frequency analysis. For this study, Easyfit software by Mathwave inc was used to perform this analysis. Easyfit is a handy utility to compute many kinds of statistical distributions off a date set in a seamlessly convenient way and without having to memorize difficult lines of code.

2.7 Calculating Return Level

The developed Cumulated Distribution Function (CDF) was used to calculate the return levels. In the CDF function variant was taken on the value equal to or less than x. The CDF probability function was expressed in an equation

$$F(x) = P\ (X \leq x)$$

The return level was calculated by using the following relationship

$$PX = P\{X \geq x\} = 1 - P\{X < x\} = 1\text{-GEV\_CDF} = 1/T$$

2.8 Computing of DDF Curves

For this study 3, 6, 12, and 24 hr frequencies were selected, and DDF relationships were developed by plotting Return level on x-axis and Rainfall Depth on y-axis. The developed scatted points were connected linearly. The formulation of the DDF relationship in MS EXCEL is shown in figure 2.3.

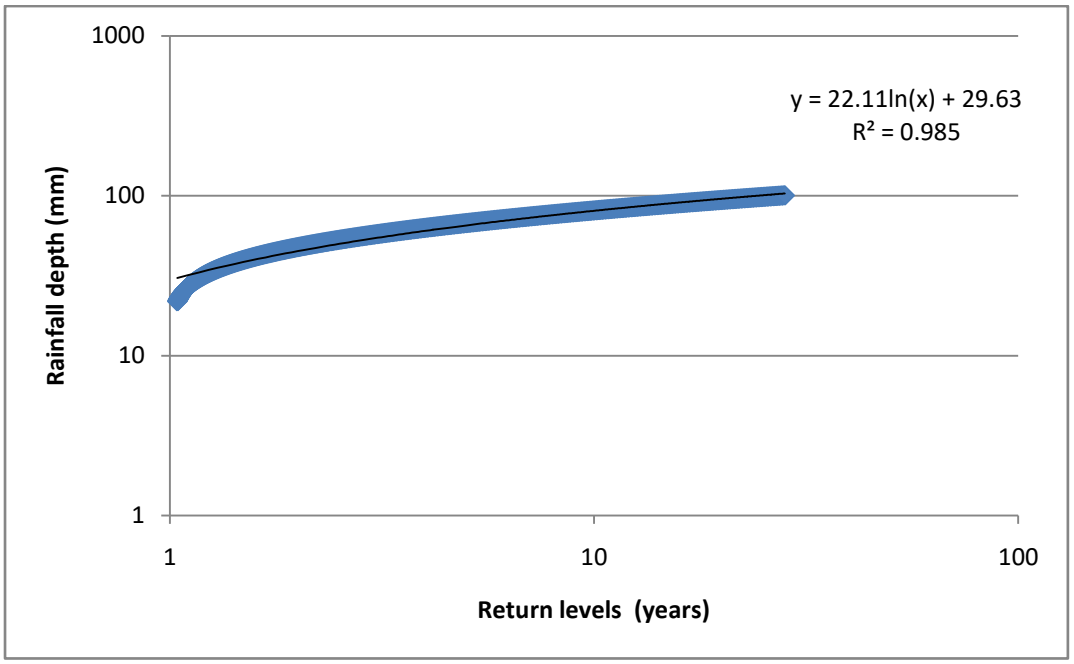

Figure 2.3: Depth Duration Frequency curve

2.9 Interpolating the DDF Curves

In this study, return levels of 2, 5, 10, 20, 30, 40, and 50 years were selected to obtain rainfall depths for the fitted frequencies i.e., 3, 6, 12, and 24 hr. After that, the depths of 3, 6, 12, and 24-hour frequencies were plotted against selected return levels for better understanding.

2.10 Critical Rainfall Depths

The rainfall depth associated with a given time interval (hourly, daily, etc.) that serves as the threshold for activating an alert level (low, medium, high, or very high) is called the critical rainfall depth. It indicates the average amount of rainfall projected to fall once during the relevant return period and is used to determine the severity of potential consequences, such as floods or infrastructure stress. In this study, four different alert levels i.e. low, medium, high, and exceptionally high, were developed based on return level. Rainfall depth of 2-year return level assigned to low alert, rainfall depth of 10-year return level assigned to medium alert, rainfall depth of 20-year return level assigned to high alert and rainfall depth of 50-year return level assigned to the exceptionally high alert.

Remittances Review
June 2024,
Volume: 9, No: 3, 2017-2037
ISSN: 2059-6588(Print) | ISSN 2059-6596(Online

3. RESULT

3.1 Evaluation of Satellite Rainfall Data

Satellite rainfall data was evaluated using GPM and TRMM monthly products by comparing with the ground rain gauge data provided by the Pakistan Meteorological Department (PMD). The scattered diagrams were developed both for TRMM and GPM and the coefficient of determination (R^2) was measured by using Linear Regression. The linear regression equations and R^2 for the two districts of Kashmir shown in Table 3.1, the R^2 values for both satellites were more than 0.75. The R^2 values remain relatively similar and there is very little variation between the two satellite data sets. Zhang et al. (2022) compared the TRMM satellite data set with the ground rain gauge data set. The authors found that the R^2 values for the monthly data set were high (0.94), as in our case, the R^2 values were also high. The maximum R^2 values were achieved in Muzaffarabad, which were 0.918, 0.912 for TRMM and GPM, respectively. This shows that both satellite data sets can be used for further analysis.

Table 3.1: Linear Regression Analysis for Satellite Rainfall Data

District	TRMM		GPM	
	Equation	R^2	Equation	R^2
Kotli	y=0.847x+15.795	0.787	y=0.842x+14.423	0.774
Muzaffarabad	y=0.905x+6.181	0.918	y=0.896x-0.304	0.912

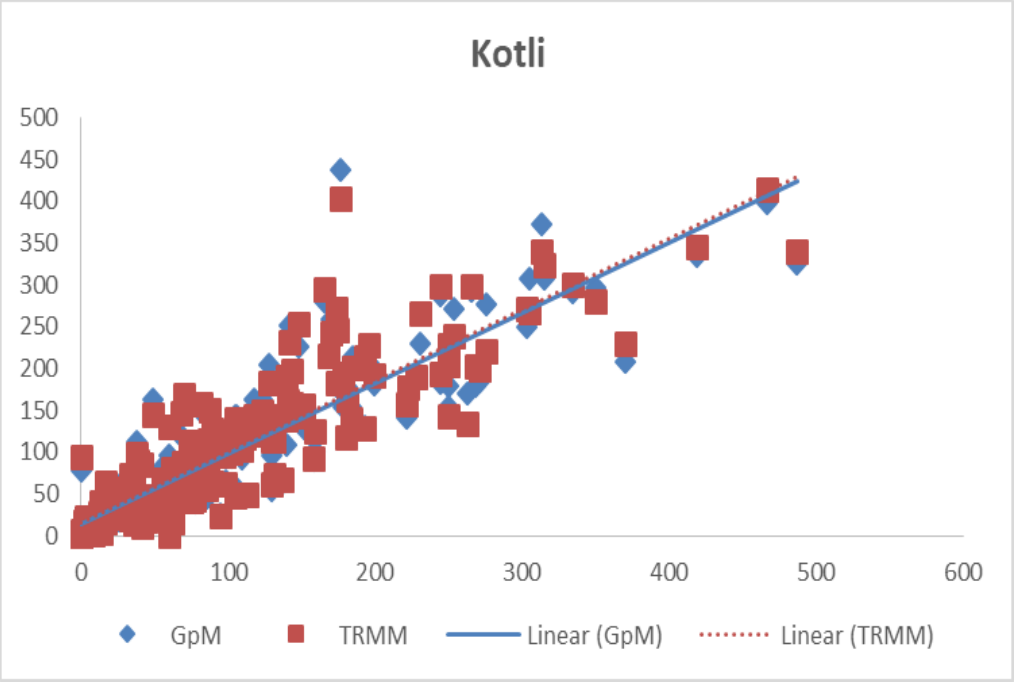

Figure 3.1: Scattered Diagram for Kotli

Remittances Review
June 2024,
Volume: 9, No: 3, 2017-2037
ISSN: 2059-6588(Print) | ISSN 2059-6596(Online

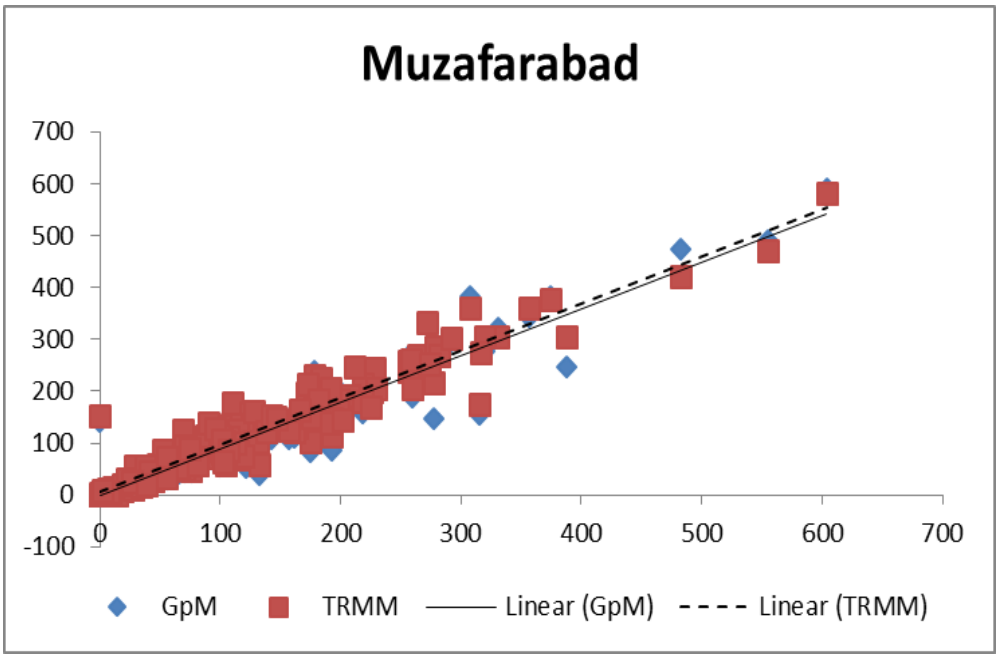

Figure 3.2:Scattered Diagram for Muzaffarabad

3.2 Statistical Parameters

The statistical evaluation of satellite data (TRMM and GPM) on a monthly basis was carried out by comparing ground rain gauge data. The Mean Error (ME), Mean Absolute Error (MAE), Root Mean Square Error (RMSE), Present bias (PBIAS), Nash-Sutcliffe Efficiency (NSE), and correlation coefficient (r) were calculated for the selected district (Table 3.2 , 3.3).Across the two selected districts, ME values varied between −5.18 and 0.73 for TRMM and between −12.67 and -1.20 for GPM. The negative values indicate that, on average, the predicted value is smaller than the actual value, and positive values indicate that the predicted values are larger than the actual values. In our case, the ME values were lower, which is in good agreement with the data. The TRMM and GPM provide the lowest ME for the Muzaffarabad district. The MAE and RMSE for the TRMM and GPM data set were maximum for Kotli district (29.09,43.41, and 29.49, 44.80) and minimum for Muzaffarabad district (18.94, 29.08, and 20.13, 32.29). These lower values of MAE and RMSE show that satellite data were closely linked with the ground data set.
The PBIAS values for the TRMM and GPM data sets were between -4.32 and 0.73 and -10.58 and -1.21, respectively. The negative values between 0-20% indicate that the model has a small under-prediction bias, and positive values between 0 to 20% show that the model has a small over-prediction bias. The PBias values under 20% mean model's predictions are acceptable (Gilewskic, P., and M. Nawalany, 2018). In our case, PBias values for both satellite data set were under 20%. The maximum and minimum values of NSE were 0.91 and 0.78 and .89 and 0.76 for TRMM and GPM data sets, respectively. If the NSE value is between 0.5 and 1.0 then model performance is satisfactory to very good (Gilewskic, P., and M. Nawalany, 2018). In our case, NSE values of all districts for both satellite data fall in the satisfactory to very good region. The Pearson's correlation coefficient (r) values of all

districts for both satellites were above 0.99. If the r value falls between 0.85 and 1.00, then model performance is very good (Gilewskic, P., and M. Nawal any, 2018). All statistical parameters indicate that the model data can be processed further.

Table 3.2: Statistical Evaluation of TRMM Data

District	TRMM					
	ME	MAE	RMSE	PBias	NSE	r
Kotli	0.731482	29.09161	43.41012	0.739339	0.782791	0.997498
Muzaffarabad	-5.18082	18.9468	29.08649	-4.32796	0.915601	0.9993

Table 3.3: Statistical Evaluation of GPM Data

District	GPM					
	ME	MAE	RMSE	PBias	NSE	r
Kotli	-1.2039	29.49478	44.80648	-1.21683	0.768593	0.999022
Muzaffarabad	-12.6714	20.13826	32.29008	-10.5854	0.895985	0.9962

3.3 Development of Depth Duration Frequency Curve (DDF)

The DDF curves were developed with GEV distribution for the district of Kashmir. The DDF curves were established for four different events such as 3, 6, 12, 24 hours (Figures 3.3) The linear regression equations were developed and its accuracy was assessed by R^2 for all district DDF curves. The R^2 values for all district was more than 0.85. This strong correlation indicates the model can be used for further analysis.

The DDF curves, equations and R^2values are given in Table 3.4 (based on TRMM) and 3.5 (based on GPM) data sets.

Table 3.4: DDF Curves Equations and R^2 values based on TRMM Data

TRMM Districts Names	3 hr	6 hr	12 hr	24 hr
Bagh	y = 6.564ln(x) + 24.20	y = 11.63ln(x) + 28.30	y = 8.367ln(x) + 35.84	y = 11.24ln(x) + 44.83
	R^2 = 0.862	R^2 = 0.941	R^2 = 0.855	R^2 = 0.983
Bhimber	y = 9.387ln(x) + 35.61	y = 12.88ln(x) + 43.90	y = 15.03ln(x) + 50.79	y = 14.20ln(x) + 56.02
	R^2 = 0.993	R^2 = 0.998	R^2 = 0.986	R^2 = 0.979
Kotli	y = 14.16ln(x) + 29.28	y = 14.76ln(x) + 38.64	y = 18.94ln(x) + 43.60	y = 23.33ln(x) + 50.40
	R^2 = 0.995	R^2 = 0.993	R^2 = 0.995	R^2 = 0.957

Mirpur	y = 17.64ln(x) + 31.95	y = 15.81ln(x) + 42.57	y = 27.32ln(x) + 39.60	y = 27.47ln(x) + 46.35
	R^2 = 0.997	R^2 = 0.941	R^2 = 0.983	R^2 = 0.984
Muzaffarabad	y = 9.566ln(x) + 16.15	y = 10.46ln(x) + 20.77	y = 9.840ln(x) + 28.60	y = 18.23ln(x) + 32.18
	R^2 = 0.947	R^2 = 0.978	R^2 = 0.963	R^2 = 0.968
Poonch	y = 10.15ln(x) + 35.1	y = 16.00ln(x) + 41.26	y = 17.43ln(x) + 44.38	y = 17.41ln(x) + 54.49
	R^2 = 0.871	R^2 = 0.949	R^2 = 0.956	R^2 = 0.991
Sadhnoti	y = 15.21ln(x) + 37.56	y = 17.86ln(x) + 47.35	y = 21.25ln(x) + 50.81	y = 22.45ln(x) + 57.22
	R^2 = 0.997	R^2 = 0.989	R^2 = 0.990	R^2 = 0.987

Table 3.5: DDF Curves Equations and R^2 values based on GPM Data

GPM Districts Names	**3 hr**	**6 hr**	**12 hr**	**24 hr**
Bagh	y = 16.01ln(x) + 20.96	y = 18.84ln(x) + 27.95	y = 35.56ln(x) + 21.48	y = 27.65ln(x) + 38.93
	R^2 = 0.992	R^2 = 0.996	R^2 = 0.981	R^2 = 0.995
Bhimber	y = 12.90ln(x) + 28.33	y = 20.15ln(x) + 39.64	y = 24.33ln(x) + 46.83	y = 22.24ln(x) + 55.62
	R^2 = 0.998	R^2 = 0.997	R^2 = 0.992	R^2 = 0.995
Kotli	y = 12.30ln(x) + 33.66	y = 13.26ln(x) + 48.44	y = 18.99ln(x) + 57.35	y = 20.13ln(x) + 60.9
	R^2 = 0.942	R^2 = 0.898	R^2 = 0.969	R^2 = 0.925
Mirpur	y = 13.18ln(x) + 40.78	y = 25.21ln(x) + 47.46	y = 24.58ln(x) + 63.34	y = 23.63ln(x) + 72.12
	R^2 = 0.997	R^2 = 0.996	R^2 = 0.998	R^2 = 0.979
Muzaffarabad	y = 11.89ln(x) + 4.515	y = 13.30ln(x) + 10.69	y = 17.84ln(x) + 15.80	y = 22.45ln(x) + 23.00
	R^2 = 0.977	R^2 = 0.991	R^2 = 0.998	R^2 = 0.992
Poonch	y = 19.97ln(x) + 18.32	y = 24.00ln(x) + 26.27	y = 25.24ln(x) + 33.98	y = 27.51ln(x) + 41.55
	R^2 = 0.985	R^2 = 0.976	R^2 = 0.995	R^2 = 0.995
Sadhnoti	y = 30.45ln(x) + 11.85	y = 35.56ln(x) + 21.48	y = 34.17ln(x) + 32.08	y = 33.41ln(x) + 40.40
	R^2 = 0.966	R^2 = 0.981	R^2 = 0.993	R^2 = 0.997

Depth duration frequency curves of the Kashmir were plotted and given in the following figures. For better understanding DDF curves for different time frequencies were plotted on the same graph for each district. It is observed that the DDF curves for all district based on TRMM and GPM shows a similar increasing pattern.

Unlike other districts, Bhimber district showed considerable variation in DDF curves for both satellites. The overlap of 12 hr and 24 hr frequency curves shows that in the Bhimber

district there must be no or slight shower of duration greater than 12 hr but below 12 hr there must have been plenty.

In Mirpur district DDF curves by TRMM data shows that 3 hr and 6 hr interval curves were overlaped in later years which indicates there were no or Slight rainfall greater than 3 hr and less than 6 hr, moreover for time intervals 6 hr and 12 hr there is a palenty of rainfall. But in GPM DDF curves similar like TRMM there is a slight difference between 12 hr and 24 hr rainfall events.

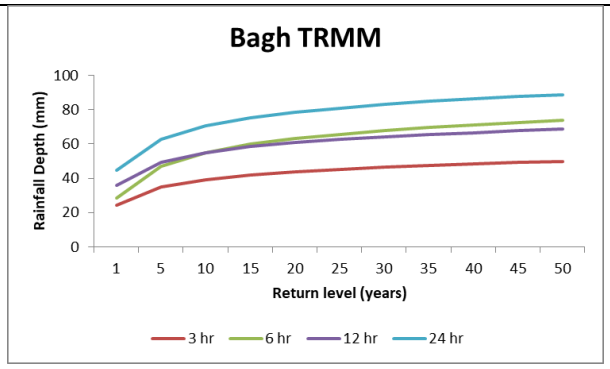

(a)

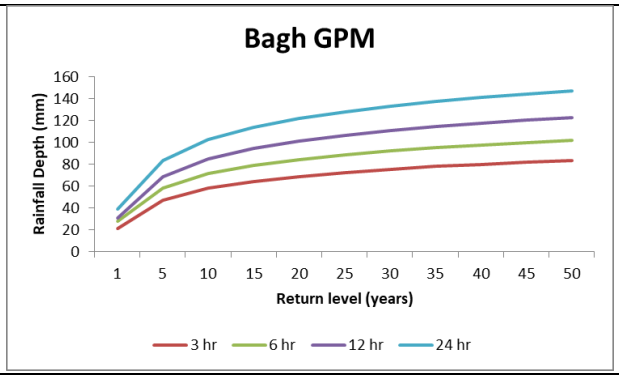

(b)

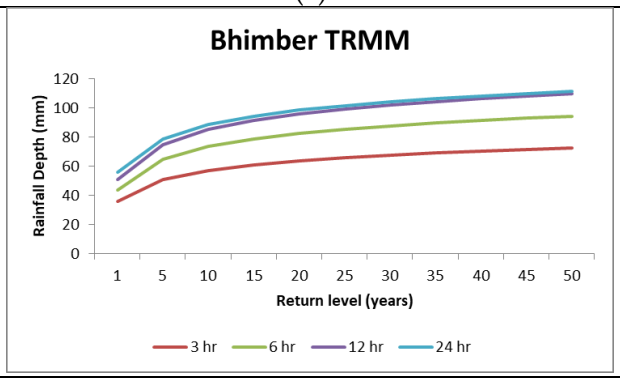

(c)

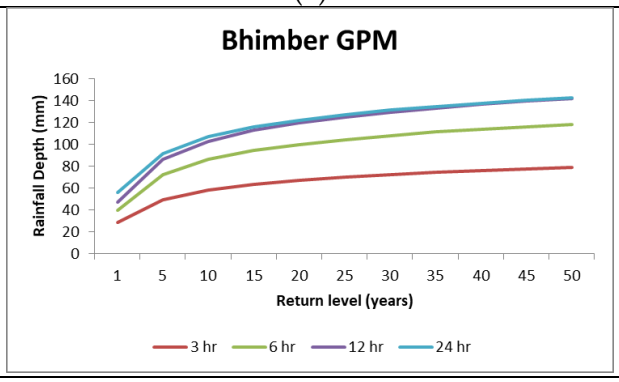

(d)

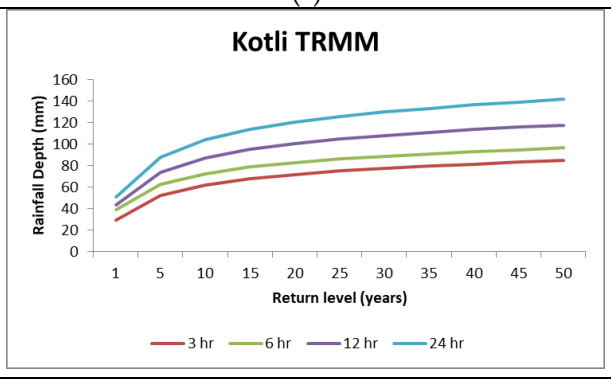

(e)

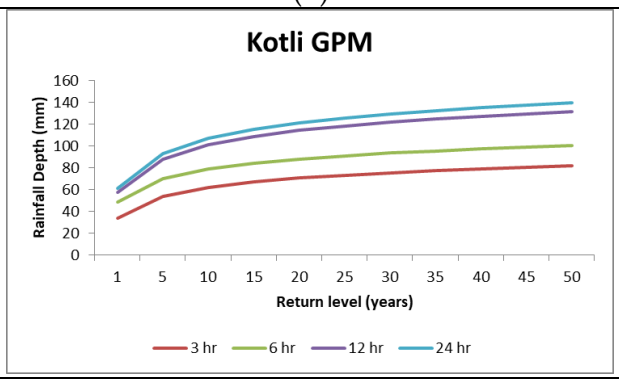

(f)

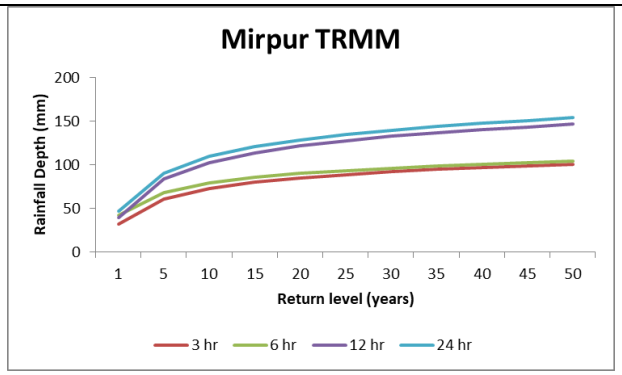

(g)

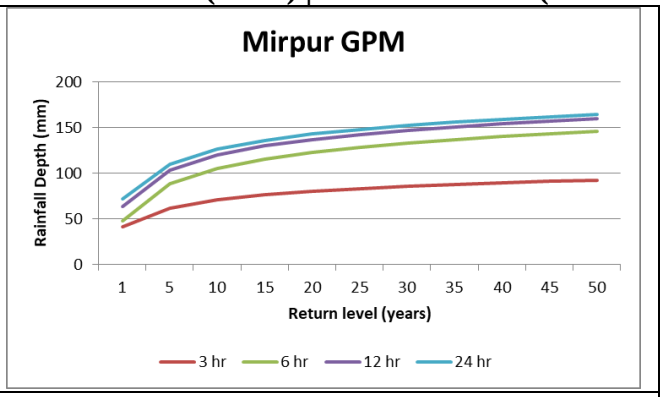

(h)

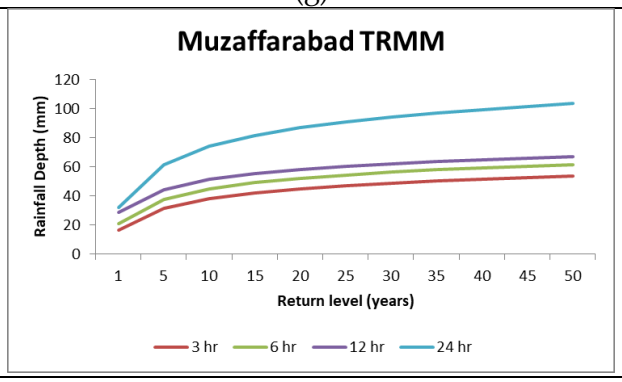

(i)

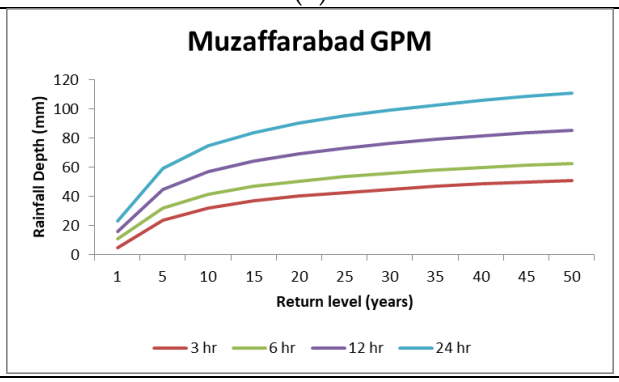

(j)

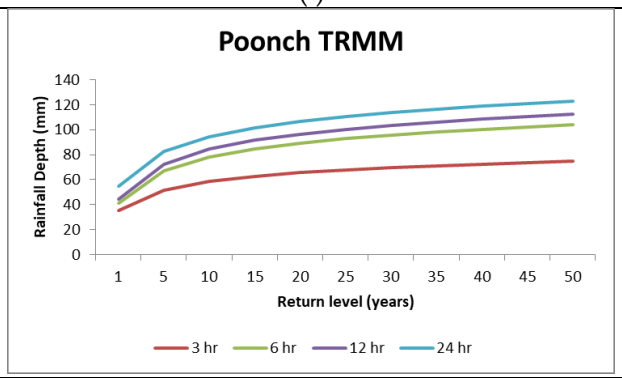

(k)

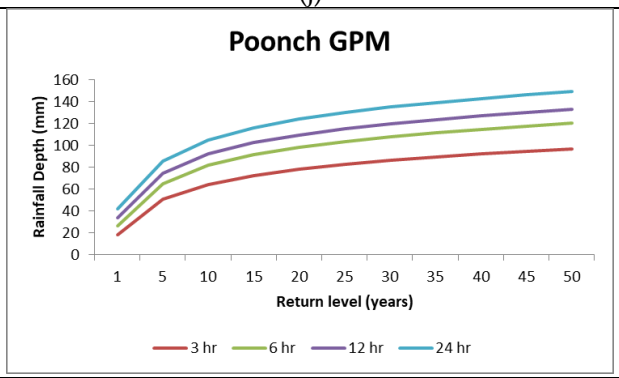

(l)

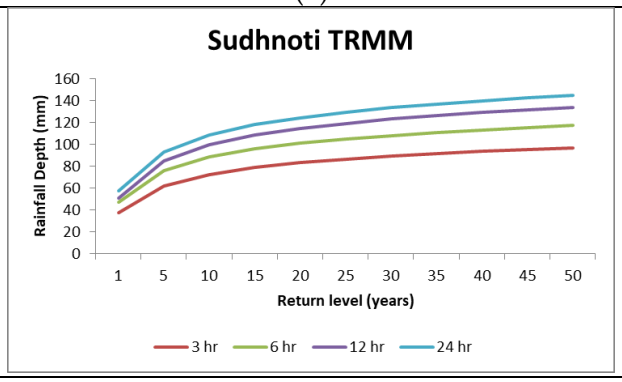

(m)

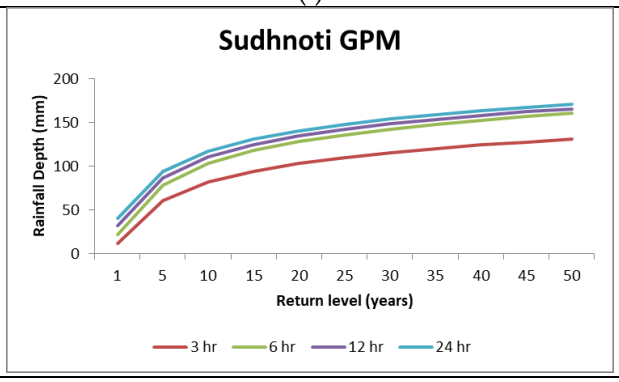

(n)

Figure 3.3**:** DDF curves for AJK Di, (a) Bagh(TRMM), (b) Bagh (GPM) (c) Bhimber (TRMM), (d) Bhimber (GPM) (e) Kotli (TRMM), (f) Kotli (GPM) (g) Mirpur (TRMM), (h) Mirpur (GPM) (i) Muzaffarabad (TRMM), (j) Muzaffarabad (GPM) (k) Poonch (TRMM), (l) Poonch (GPM) (m)

Sudhnoti(TRMM), (n) Sudhnoti(GPM)

3.4 Critical Rainfall Depths for Azad Jammu Kashmir

Table 3.6 shows the critical rainfall depth ofKashmir. Muzafarabad (Jammu Kashmir) the exceptionally high rainfall depth predicted by the model for GPM is 51.02 mm and 110.8 mm for 3 hr and daily storm frequencies, respectively. In the Kashmir region results showed that theexceptionally high critical rainfall depth for 3 hr and 24 hr frequencies recorded for Sudhnoti was 130.9mm, and 171.1 mm respectively. Result indicated that there was small difference between the critical rainfall depths for 3 hr and 24 hr frequencies which indicates that Sudhnoti receives the short interval rainfall with high intensity.

Table 3.6: Critical rainfall for the AJK

District		GPM				TRMM			
		Low	MED	High	EX. High	Low	MED	High	EX. High
Bagh	3 hr	32.05	57.82	68.92	83.59	28.74	39.31	43.86	49.87
	6 hr	41.00	71.33	84.38	101.6	36.36	55.07	63.14	73.79
	12 hr	47.11	84.85	101.1	122.5	41.63	55.10	60.90	68.57
	24hr	58.09	102.5	121.7	147.0	52.62	70.71	78.50	88.80
Bhimber	3 hr	37.27	58.03	66.97	78.79	42.11	57.22	63.73	72.33
	6 hr	53.60	86.03	100.0	118.4	52.82	73.55	82.48	94.28
	12 hr	63.69	102.8	119.7	142.0	61.20	85.39	95.81	109.5
	24 hr	71.03	106.8	122.2	142.6	65.86	88.71	98.55	111.5
Kotli	3 hr	42.18	61.98	70.50	81.77	39.09	61.88	71.69	84.67
	6 hr	57.63	78.97	88.16	100.3	48.87	72.62	82.85	96.38
	12hr	70.51	101.0	114.2	131.6	56.72	87.21	100.3	117.6
	24 hr	74.85	107.2	121.2	139.6	66.57	104.1	120.2	141.6
Mirpur	3 hr	49.91	71.12	80.26	92.34	44.17	72.56	84.79	100.9
	6 hr	64.93	105.5	122.9	146.0	53.52	78.97	89.93	104.4
	12 hr	80.37	119.9	136.9	159.4	58.53	102.5	121.4	146.4
	24 hr	88.49	126.5	142.9	164.5	65.39	109.6	128.6	153.8
Muzaffarabad	3 hr	12.75	31.89	40.13	51.02	22.78	38.17	44.80	53.57
	6 hr	19.90	41.31	50.53	62.71	28.02	44.85	52.10	61.68
	12 hr	28.16	56.87	69.24	85.59	35.42	51.25	58.07	67.09
	24 hr	38.56	74.69	90.25	110.8	44.81	74.15	86.79	103.4
Poonch	3 hr	32.16	64.30	78.14	96.44	42.13	58.47	65.50	74.80
	6 hr	42.90	81.53	98.16	120.1	52.35	78.10	89.19	103.8
	12 hr	51.47	92.09	109.5	132.7	56.46	84.51	96.59	112.5
	24 hr	60.61	104.8	123.9	149.1	66.55	94.57	106.6	122.5
Sudhnoti	3 hr	32.95	81.96	103.0	130.9	48.10	72.58	83.12	97.06
	6 hr	46.12	103.3	128.0	160.5	59.72	88.47	100.8	117.2
	12 hr	55.76	110.7	134.4	165.7	65.53	99.73	114.4	133.9
	24 hr	63.55	117.3	140.4	171.1	72.78	108.9	124.4	145.0

4. Discussion

This study evaluated the applicability of satellite-derived precipitation products (TRMM and GPM) for developing Depth–Duration–Frequency (DDF) curves and defining critical rainfall thresholds in the data-scarce, mountainous region of Kashmir. The results demonstrate that satellite rainfall products, when appropriately validated and statistically processed, can serve as reliable substitutes for sparse rain gauge networks in complex terrains.

4.1 Performance of Satellite Rainfall Estimates

The comparison between satellite-derived rainfall (TRMM and GPM) and ground-based rain gauge observations revealed strong agreement across the study districts. Coefficients of determination ($R^2 > 0.77$ for all districts) indicate that both satellite products capture the temporal variability of precipitation reasonably well. The slightly higher R^2 values observed for TRMM in Kotli and Muzaffarabad are consistent with earlier findings showing that TRMM performs particularly well in tropical and subtropical mountainous regions (Huffman et al., 2007; Kummerow et al., 2000).

Statistical indicators such as MAE, RMSE, PBIAS, NSE, and Pearson's r further confirm the suitability of the satellite datasets. The NSE values between 0.76 and 0.91 fall within the "satisfactory to very good" range, suggesting robust model performance (Moriasi et al., 2007; Gilewski &Nawalany, 2018). The consistently high correlation coefficients ($r > 0.99$) indicate that satellite data reliably track rainfall patterns despite inherent uncertainties related to sensor limitations, orographic effects, and retrieval algorithms.

The slight underestimation observed (negative PBIAS values, mostly $< -10\%$) is a known limitation of satellite products in regions with intense orographic precipitation and shallow stratiform rainfall, where microwave and infrared retrieval algorithms may underestimate rainfall intensity (Islam, 2013; Vernimmen et al., 2012). Nevertheless, since the bias remains within acceptable limits ($< 20\%$), the satellite data are considered appropriate for hydrological and climatological applications in AJK.

4.2 Applicability of GEV Distribution for Extreme Rainfall Modeling

The use of the Generalized Extreme Value (GEV) distribution for modeling extreme rainfall events proved effective for all studied durations (3, 6, 12, and 24 hours). The GEV distribution is widely recognized for its flexibility in modeling extreme hydrological events and has been successfully applied in flood frequency and rainfall extremes studies worldwide (Coles, 2001; Katz et al., 2002).

The high goodness-of-fit reflected in the strong R^2 values (> 0.85) for all DDF regressions suggests that the GEV model adequately represents the statistical behavior of extreme rainfall in the study area. This is particularly important in a climate-sensitive region like

AJK, where rainfall extremes are influenced by monsoon variability, western disturbances, and complex topography.

The ability of the GEV distribution to account for heavy-tailed behavior is especially relevant for districts such as Sudhnoti and Mirpur, where short-duration rainfall exhibits very high intensities. Such patterns are consistent with findings from other monsoon-dominated regions, where short, intense rainfall bursts contribute significantly to flash flooding and landslide hazards (Zhang & Zhou, 2015; Piman et al., 2016).

4.3 Interpretation of DDF Curves Across Districts

The developed DDF curves show a consistent increase in rainfall depth with increasing return period and duration, which aligns with hydrological theory and previous empirical studies (Chow et al., 1988; Koutsoyiannis et al., 1998). However, notable spatial variations exist among districts due to differences in elevation, exposure to monsoon flows, and local climatic conditions.

For instance, Sudhnoti exhibited the highest short-duration rainfall intensities, suggesting a high susceptibility to flash floods and surface runoff generation. In contrast, Muzaffarabad showed comparatively lower rainfall depths, which may be attributed to its topographic position and rain-shadow effects.

The overlapping of certain duration curves (e.g., 12 hr and 24 hr in Bhimber, and 3 hr and 6 hr in Mirpur) indicates that rainfall in these districts tends to occur in short, intense bursts rather than prolonged events. This behavior is critical for urban drainage design, slope stability assessments, and early warning systems, as short-duration rainfall often produces more severe hydrological responses than longer, moderate events (Zhang et al., 2022).

4.4 Critical Rainfall Thresholds and Risk Implications

The classification of rainfall thresholds into low, medium, high, and exceptionally high alert levels based on return periods provides a practical framework for disaster risk management. The exceptionally high thresholds (50-year return period) highlight districts such as Sudhnoti and Mirpur as high-risk zones for extreme rainfall and potential flooding.

The small difference between short-duration (3 hr) and daily (24 hr) extreme rainfall depths in Sudhnoti suggests that intense convective storms dominate precipitation there. This has serious implications for flash flood generation, soil erosion, and landslide triggering, especially in steep terrains with limited infiltration capacity.

Such findings reinforce the importance of incorporating high-resolution satellite rainfall data into early warning systems, particularly in regions where ground-based monitoring is insufficient or unreliable. Satellite data provide near-real-time coverage and enable rapid risk assessment during extreme weather events (Prakash, 2019).

4.5 Implications for Climate Change Adaptation and Water Resources Management

The results confirm that satellite-derived precipitation products can play a critical role in climate change adaptation strategies, flood forecasting, infrastructure design, and agricultural planning in data-scarce regions. As climate change intensifies rainfall variability

and increases the frequency of extreme events, traditional design standards based solely on historical gauge data may no longer be adequate (IPCC, 2021; Hanif et al., 2013).

The integration of satellite rainfall, extreme value statistics, and DDF analysis provides a cost-effective and scalable approach for updating hydrological design standards and risk maps in vulnerable regions such as Kashmir.

5. **Conclusion**

Satellite data were evaluated with the ground rain gauge data by finding the R^2 values and other statistical parameters for both satellites. Results showed that R^2 values for the TRMM data are slightly higher than the GPM data, which shows that the GPM data overestimates rainfall over maximum points in the country. Other statistical parameters also showed significant results, which showed the agreement between rain gauge and satellite data. DDF curves were developed for all districts of Kashmir for four different durations of annual rainfall. Maximum results showed that the R^2 value for the maximum districts was more than 0.95, and in some districts between 0.85 and 0.95.

6. Recommendations

- It is recommended that satellite rainfall data is a good alternative for theground rain gauge data for the area where no or very low network of rain gauge stations is available.
- Critical rainfall values developed in this study can be used for the real time flood alertfor better flood alerts and other management practices.

***Conflict of Interest*:** The Authors declare that there is no conflict of interest.

Authors' Contribution Statements: Remotely sensed rainfall estimates can play a vital role inon-farm water management, flood management systems, and water resources management. Remotely sensed rainfall estimatesdata have significant potential to overcome the scarcity of rainfall measurement data with more accuracy and easy access.

7. References

Coles, S. (2001). *An introduction to statistical modeling of extreme values*. Springer.

Franchito, S. H., Rao, V. B., Vasques, A. C., Santo, C. M. E., & Conforte, J. C. (2009). Validation of TRMM precipitation radar monthly rainfall estimates over Brazil. *Journal of Geophysical Research: Atmospheres, 114*, D02105. https://doi.org/10.1029/2008JD010613

Gilewski, P., &Nawalany, M. (2018). Inter-comparison of rain-gauge, radar, and satellite (IMERG-GPM) precipitation estimates performance for rainfall–runoff modeling in a mountainous catchment in Poland. *Water, 10*(9), 1–23. https://doi.org/10.3390/w10091234

Hanif, M., Khan, A. H., & Adnan, S. (2013). Latitudinal precipitation characteristics and trends in Pakistan. *Journal of Hydrology, 492*, 266–272. https://doi.org/10.1016/j.jhydrol.2013.04.013

Huffman, G. J., Adler, R. F., Bolvin, D. T., Gu, G., Nelkin, E. J., Bowman, K. P., Hong, Y., Stocker, E. F., & Wolff, D. B. (2007). The TRMM multi-satellite precipitation analysis (TMPA): Quasi-global, multiyear, combined-sensor precipitation estimates at fine scales. *Journal of Hydrometeorology, 8*(1), 38–55. https://doi.org/10.1175/JHM560.1

Huffman, G. J., Bolvin, D. T., & Nelkin, E. J. (2017). *Integrated Multi-satellite Retrievals for GPM (IMERG) technical documentation* (Version 4.6). NASA.

Islam, M. N. (2013). Evaluation of TRMM rainfall products for hydrological uses at different scales [Master's thesis, UNESCO-IHE Institute for Water Education].

Katz, R. W., Parlange, M. B., &Naveau, P. (2002). Statistics of extremes in hydrology. *Advances in Water Resources, 25*(8–12), 1287–1304. https://doi.org/10.1016/S0309-1708(02)00056-8

Koutsoyiannis, D., Kozonis, D., & Manetas, A. (1998). A mathematical framework for studying rainfall intensity–duration–frequency relationships. *Journal of Hydrology, 206*(1–2), 118–135. https://doi.org/10.1016/S0022-1694(98)00097-3

Kummerow, C., Barnes, W., Kozu, T., Shiue, J., & Simpson, J. (1998). The Tropical Rainfall Measuring Mission (TRMM) sensor package. *Journal of Atmospheric and Oceanic Technology, 15*(3), 809–817.https://doi.org/10.1175/1520-0426(1998)015<0809:TTRMMS>2.0.CO;2

Kummerow, C., Simpson, J., Thiele, O., Barnes, W., Chang, A. T. C., Stocker, E., Adler, R. F., Hou, A., Kakar, R., Wentz, F., Ashcroft, P., Kozu, T., Hong, Y., Okamoto, K., Iguchi, T., Kuroiwa, H., Im, E., Haddad, Z., Huffman, G., Ferrier, B., Olson, W. S., & Wilheit, T. T. (2000). The status of the Tropical Rainfall Measuring Mission (TRMM) after two years in orbit. *Journal of Applied Meteorology, 39*(12), 1965–1982. https://doi.org/10.1175/1520-0450(2001)040<1965:TSOTTR>2.0.CO;2

Li, M., & Shao, Q. (2010). An improved statistical approach to merge satellite rainfall estimates and raingauge data. *Journal of Hydrology, 385*(1–4), 51–64. https://doi.org/10.1016/j.jhydrol.2010.02.005

Moriasi, D. N., Arnold, J. G., Van Liew, M. W., Bingner, R. L., Harmel, R. D., & Veith, T. L. (2007). Model evaluation guidelines for systematic quantification of accuracy in watershed simulations. *Transactions of the ASABE, 50*(3), 885–900. https://doi.org/10.13031/2013.23153

Piman, T., Pawattana, C., Vansarochana, A., Aekakkararungroj, A., &Hormwichian, R. (2016). Analysis of historical changes in rainfall in Huai Luang Watershed, Thailand. *International Journal of Technology, 7*(7), 1155–1162. https://doi.org/10.14716/ijtech.v7i7.430

Prakash, S. (2019). Performance assessment of CHIRPS, MSWEP, SM2RAIN-CCI, and TMPA precipitation products across India. *Journal of Hydrology, 571*, 50–59.

https://doi.org/10.1016/j.jhydrol.2019.01.036

Vernimmen, R. R. E., Hooijer, A., Mamenun, Aldrian, E., & van Dijk, A. I. J. M. (2012). Evaluation and bias correction of satellite rainfall data for drought monitoring in Indonesia. *Hydrology and Earth System Sciences, 16*, 133–146. https://doi.org/10.5194/hess-16-133-2012

Zhang, L., & Zhou, T. (2015). Drought over East Asia: A review. *Journal of Climate, 28*(8), 3375–3393. https://doi.org/10.1175/JCLI-D-14-00259.1

Zhang, Y., Wu, C., Yeh, P. J. F., Li, J., Hu, B. X., Feng, P., & Jun, C. (2022). Evaluation and comparison of precipitation estimates and hydrologic utility of CHIRPS, TRMM 3B42 V7 and PERSIANN-CDR products in various climate regimes. *Atmospheric Research, 265*, 105888. https://doi.org/10.1016/j.atmosres.2021.105888